OPEN ACCESS Freely available online

PLOS ONE

Faster Metabolite ^{1}H Transverse Relaxation in the Elder Human Brain

Małgorzata Marjańska*, Uzay E. Emir¤, Dinesh K. Deelchand, Melissa Terpstra

Center for Magnetic Resonance Research and Department of Radiology, University of Minnesota, Minneapolis, Minnesota, United States of America

Abstract

^{1}H magnetic resonance spectroscopy (MRS) is unique among imaging modalities because signals from several metabolites are measured during a single examination period. Each metabolite reflects a distinct intracellular process. Furthermore transverse (T_2) relaxation times probe the viability of the cell microenvironment, e.g., the viscosity of the cellular fluids, the microscopic susceptibility distribution within the cells, and the iron content. In this study, T_2*s* of brain metabolites were measured in the occipital lobe of eighteen young and fourteen elderly subjects at a field strength of 4 tesla. The T_2*s* of *N*-acetylaspartate, total creatine, and total choline were 23%, 16% and 10% shorter in elderly than in young subjects. The findings of this study suggest that noninvasive detection of T_2 provides useful biological information on changes in the cellular microenvironment that take place during aging.

Citation: Marjańska M, Emir UE, Deelchand DK, Terpstra M (2013) Faster Metabolite ^{1}H Transverse Relaxation in the Elder Human Brain. PLoS ONE 8(10): e77572. doi:10.1371/journal.pone.0077572

Editor: Zhuoli Zhang, Northwestern University Feinberg School of Medicine, United States of America

Received May 15, 2013; **Accepted** September 3, 2013; **Published** October 2, 2013

Funding: This work was supported by the National Institutes of Health through grants R21 AG029582, RO1 AG039396, P41 RR008079, P41 EB015894, P30 NS057091, P30 NS507608, S10 RR023730. The funders had no role in study design, data collection and analysis, decision to publish, or preparation of the manuscript.

Competing interests: The authors have declared that no competing interests exist.

* E-mail: gosia@cmrr.umn.edu

¤ Current address: FMRIB Centre, Department of Clinical Neurology, University of Oxford, Headington, Oxford, UK

Introduction

^{1}H magnetic resonance spectroscopy (MRS) is unique among imaging modalities because signals from several metabolites are measured during a single examination period [1]. Each observable metabolite is associated with a distinct set of intracellular processes since the metabolites are primarily located in the intracellular compartment of the brain [1,2]. Some metabolites are preferentially concentrated in certain cell types and in different parts of the cell. *N*-acetylaspartate (NAA) is located primarily in neuronal cell bodies, axons, and dendrites, and is considered to be a sensitive marker for neuronal density or viability. Total creatine (tCr, creatine with phosphocreatine) and choline containing compounds (tCho, phosphorylcholine (PCho) and glycerophosphorylcholine (GPC)) are present both in neuronal and glial cells [1]. NAA and tCr are located in the cytoplasm [1,3,4], and tCho in the cytoplasm and cellular membrane [5]. Therefore, abnormal concentrations of specific metabolites may reflect particular aspects of neurodegenerative processes at molecular and cellular levels. However, detection of static metabolite concentrations alone provides only a partial description of viability.

Transverse relaxation results from nuclear spin-spin interactions and is sensitive to changes in molecular motion, mainly through interaction of metabolites with structural or cytosolic macromolecules [6,7]. Previous MRS studies of transverse relaxation time constants (T_2s) of cerebral metabolites have observed changes induced by pathology or naturally occurring processes during development [6–9]. Hence, T_2s of metabolites could be used to probe the cellular microenvironment e.g., the viscosity of the cellular fluids, the microscopic susceptibility distribution within cells, and the iron content. As such, investigation of the T_2s of several metabolites has high potential for early stage sensitivity to processes that take place during aging. Another advantage of assessing the dynamic parameter, T_2, is that it is not susceptible to signal normalization which can confound the MRS measurement of static concentration.

Most studies in humans have focused on measurement of the T_2 of singlet resonances due to the relative experimental simplicity. In a handful of studies related to aging, T_2 values have been measured for singlets of NAA, tCr, and tCho with contradicting results [10–13]. Among those, one study of the centrum semiovale that utilized a linewidth based approach and has not been validated or adopted since publication [12] found a longer T_2 of NAA in elderly. A separate study of the occipital cortex that was complicated by overlap among water and metabolite signals [10] did not find any age associated differences in T_2. The two remaining studies found no age

dependence in the frontal lobe [13], and shorter T_2s of NAA, tCr, tCho in the occipital cortex as well as other brain regions of elderly than adolescent subjects [11]. Most of these studies were performed at 1.5 T [10,12,13] while one was performed at 3 T [11]. All four studies were performed in a small number of subjects (at most 10 subjects per group) and with various techniques. While age associated T_2 dependence could be brain region specific, the discrepancies among current findings warrant further study of this phenomenon.

The aim of this study was to measure metabolite T_2s in a larger cohort of cognitively healthy young and elderly subjects than has been studied previously. Study of the occipital cortex facilitated examination of normal aging without confounding by pre-symptomatic presence of the most prevalent neurodegenerative conditions that impact other brain regions [14,15]. Data in this study were measured at a higher magnetic field, i.e., 4 T, which provides higher signal to noise ratio (SNR) and better spectral dispersion which leads to less overlap among resonances. Further SNR improvement was achieved using a dual loop receiver that could be used to study this superficial brain region. Additionally, each T_2 was characterized using a larger number of echo times (T_Es) than previously applied, and shorter T_Es were sampled. Spectra were fitted and quantified using LCModel for robust characterization of the signal strength, and the macromolecule contributions were taken into account. Monte Carlo simulations were performed to assess the extent to which the measured T_2 could be biased by the T_Es utilized.

Materials and Methods

1: Study population

Eighteen young (6 males, age 20 ± 1 (mean ± standard deviation (SD)) years, age range 18 to 22 years) and 14 elderly (7 males, age 77 ± 5 years, age range 70 to 80 years) individuals gave informed consent for this study, which was conducted according to the procedures approved by the Human Subjects' Protection Committee at the University of Minnesota. Candidates with neurological disorders or chronic diseases were excluded. All recruited subjects provided written informed consent. The informed consent procedure included making clear to the participant that they did not have to be in this study in order to get treatment or benefits. We also made the voluntary nature of this study clear. It was not possible to deny any potential participant treatment or other advantages associated with this study because there were no treatments or benefits associated with this study (especially considering that the vitamin C was not given because it was associated with a different phase of the experimental design that was not completed per interim research findings and funding limitations). There was no direct or societal benefit to participation in this study. The Montreal Cognitive Assessment (MoCA) was administered to detect mild cognitive impairment with high sensitivity [16]. To detect more subtle changes, timed performances on the symbol digit modalities test (DSMT, Psychological Assessment Resources, Inc., FL, USA) and on the Trail Making Test (TMTA and TMTB) were also evaluated. Each subject completed the 30 question Geriatric Depression Scale (GDS) [17]. Average scores of young participants on cognitive tests were: 28 tasks completed successfully on the MoCA, 19 s on TMTA, 43 s on TMTB, 62 digits identified on the DSMT and 2 "yes" answers on the GDS. Average scores of elderly participants were: 27 on MoCA, 33 s for TMTA, 91 s for TMTB, 41 digits on the DSMT, and 3 "yes" answers on the GDS. As such, the young and elderly participants performed similarly on the MoCA and were not depressed, while the elderly subjects completed the timed tasks more slowly as expected.

2: MR acquisition

MR acquisitions were performed using a 4-T, 90-cm bore magnet (Oxford Magnet Technology, Oxford, UK) interfaced to Varian INOVA console (Varian, Palo Alto, CA). The magnet was equipped with a Sonata gradient coil (Siemens, Erlangen, Germany), which was capable of reaching 40 mT/m in 400 μs. A quadrature 169 MHz ^{1}H surface radiofrequency (RF) coil was used to transmit and receive [18].

Each subject was positioned supine in the horizontal bore magnet with the RF coil subjacent to their occipital lobe. To ensure consistency in positioning, the external occipital protuberance, the bridge of the nose and the midline of the chin were used to define the median plane, which was centered in the bore such that midline of the brain was parallel to the axis of the magnet.

Localizer T_2-weighted multislice rapid acquisition with relaxation enhancement (RARE) images [19] (repetition time (T_R) = 4 s, T_E = 60 ms, echo train length = 8, matrix = 256x 128, slice thickness = 2 mm, 5 slices) were acquired to select a cubic volume of interest (VOI: 3 x 3 x 3 cm^3) centered on the midsagittal plane in the occipital lobe. Linewidths of 12 ± 1.5 Hz for water were obtained in both groups with no significant difference between the groups after the adjustment of all first- and second-order shim currents using the fast automatic shimming technique by mapping along projections with echo planar imaging readout (FAST(EST)MAP) [20,21].

Spectra were acquired using the stimulated echo acquisition mode (STEAM) sequence [22,23] with water suppression via variable-power RF pulses with optimized relaxation delays (VAPOR) and outer volume saturation [24]. Spectra were collected at the following seven T_Es: 10, 20, 30, 40, 60, 80, and 180 ms. Four averages were obtained for each T_E with a repetition time (T_R) of 4.5 s and STEAM mixing time of 42 ms. Additionally, unsuppressed water spectra were acquired from each subject at the following T_Es: 5, 10, 20, 30, 50, 100, 200, 400, 800, 1500, 3000, 5000 ms with T_R of 15 s. Spectra were acquired with 6,144 complex points and a spectral width of 6 kHz. Macromolecule (MM) spectra were measured from two subjects using the inversion-recovery (metabolite-nulled) technique [25] at all T_Es except 180 ms, at which T_E the MM signal was too weak for observation (T_R = 2 s, inversion time (T_I) = 0.69 s, 64 averages for T_Es 10, 20, 30, and 40 ms, 128 averages for T_Es 60, and 80 ms].

3: Spectral processing and fitting

MR spectra were analyzed using LCModel version 6.1-4A [26,27] (Stephen Provencher, Inc., Oakville, Ontario, Canada).

The basis set for LCModel was generated using home-written Matlab (The MathWorks, Inc., Natick, MA, USA) simulations based on the density matrix formalism [28] and known chemical shifts and *J*-coupling constants [29,30]. The simulated spectra of the following twenty one metabolites were included in the basis set: alanine (Ala), ascorbate (Asc), aspartate (Asp), creatine (Cr), γ-aminobutyric acid (GABA), glucose (Glc), glutamine (Gln), glutamate (Glu), glycerophosphorylcholine (GPC), glycine (Gly), glutathione (GSH), lactate (Lac), *myo*-inositol (*m*Ins), N-acetylaspartate (NAA), *N*-acetylaspartylglutamate (NAAG), phosphocreatine (PCr), phosphorylcholine (PCho), phosphorylethanolamine (PE), scyllo-inositol (*s*Ins), taurine (Tau) and threonine (Thr). Five metabolites, NAA, Cr, PCr, PCho, and GPC were separated into constituent singlet and multiplet moieties. Flags were set for calculation of tCr, i.e. combined singlet moieties of Cr and PCr, and tCho, i.e. combined singlet resonances of PCho and GPC. The occipital cortex MM spectra (average from two subjects) measured at all T_E except 180 ms (i.e. whence the MM signals were negligible) were included in the basis set.

No baseline correction, zero-filling or line broadening were applied to the *in vivo* data before input into LCModel. The fitting parameter that controls the flatness of the spline baseline function (DKNTMN) was set to 0.25, and spectra were fitted over the 0.5 to 4.2 ppm range.

4: T_2 and CSF analysis

The T_2 values were determined by fitting the metabolite concentrations obtained from LCModel analysis (without water scaling) as a function of T_E using a two parameter, mono-exponential decay function with a nonlinear least square algorithm in Matlab. The T_2 fitting was only performed on metabolite concentrations that were estimated reliably (i.e. the Cramer-Rao lower bound (CRLB) estimate of percent standard deviation of the concentration was less than 30%) at all seven T_Es. The integrals of unsuppressed water spectra were fitted with biexponential decay function with free parameters being T_2 of tissue water and cerebrospinal fluid (CSF) content of the VOI [31].

5: Monte Carlo simulations

Monte Carlo simulations were used to test for bias in calculating T_2s from spectra that were measured in this study. As such, for each measured T_2, signal strengths were computed theoretically at all T_Es used in *in vivo* experiments as well as at the additional T_Es that were not studied *in vivo* (120, 250, 400 ms). To account for the actual SNR of the experimental *in vivo* spectra, the random noise utilized in each Monte Carlo simulation was based on the maximum residual between measured *in vivo* data points and fitted T_2 curves. For each of 500 iterations per T_2, random noise (constrained to the maximum % T_2 fit residual measured per metabolite and age group from the experimental data) was added to the theoretically computed signal intensity at each T_E, and T_2 was fitted to the noised points with the two-parameter, single-exponential function. The associated SD was also determined based on the goodness of the nonlinear fit.

6: Statistical analysis

Statistical analysis was conducted using SAS Software for Windows (version 9.1, SAS Institute, Cary, NC, USA). Normal distribution could not be assumed due to heteroscedasticity, therefore a nonparametric test was chosen for analysis. The T_2 relaxation times of each metabolite and tissue water were compared between young and elderly cohorts using a Wilcoxon two sample test. The findings were considered significant if $p < 0.05$. No attempt was made to correlate T_2s with age or cognitive status due to the narrow range in age and cognitive scores.

Results

Representative ^{1}H spectra obtained at all seven T_Es from one young and one elderly subject are shown along with the position of the VOI in Figure 1. The CSF content of the VOI was significantly different between elderly and young subjects (25 ± 11% vs. 9 ± 3%, $p < 0.0001$). The excellent spectral quality that was achieved in all subjects was characterized by high SNR, narrow linewidths, absence of contamination form signals outside the voxel, and effective water suppression. Changes in resonance intensities and patterns can be observed as a function of T_E for both young and elderly subjects. The singlet resonances such as NAA at 2.01 ppm, tCr at 3.03 ppm, and tCho at 3.2 ppm become smaller with increasing T_E whereas the multiplet resonances not only become smaller but also undergo *J*-modulation. The decay of singlet signal intensity with increasing T_E is more pronounced in the elderly subject than the young subject. For better visualization of this phenomenon, the vertical scale has been adjusted such that singlet NAA resonance measured at T_E = 10 ms in both the young and the elderly subject has the same intensity. The horizontal dashed lines clarify that the NAA and tCr intensities are lower for elderly subject than the young subject at T_Es of 40 and 180 ms. The faster signal decay reflects a shorter T_2.

Representative T_2 exponential fits for the singlet NAA, tCr and tCho resonances in one young and one elderly subject are shown in Figure 2. These are the only metabolites in the basis set that satisfied quality control criteria. All fits were of good quality with R^2 values (indicators of the accuracy of the exponential fits) ≥ 0.918. The elderly curves fall below the young curves for all three metabolites illustrating the consistently faster relaxation in the elderly subject. The extent to which signal intensity drops off more quickly and to a larger extent is most apparent for NAA, demonstrating the greatest difference between elderly and young T_2s for NAA among the three metabolites. The fit of the tCho data to exponential decay was not as good as for other compounds, leading to a lower precision in measuring T_2.

Table 1 summarizes T_2 values of NAA, tCr, tCho, and tissue water for all subjects. The T_2s were significantly shorter using a one-sided probability distribution in elderly than the young subjects by 23%, 16% and 10% for NAA, tCr, tCho, respectively. When a two-sided probability distribution was used, the difference in the T_2 of tCho between young and elderly subjects did not reach significance. Additionally, T_2 of

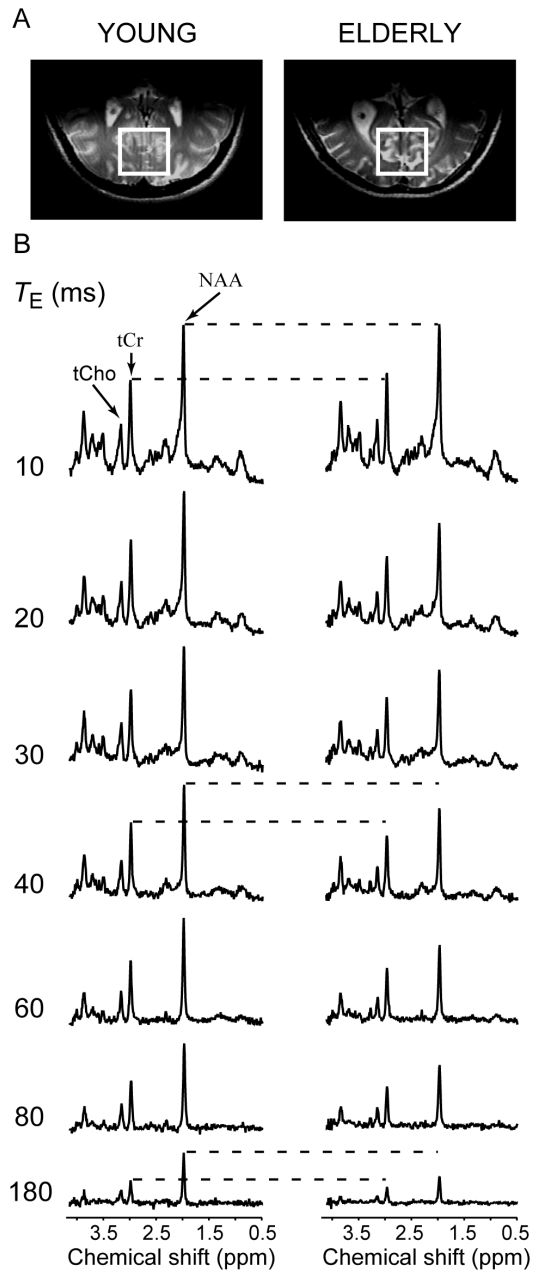

Figure 1. Voxel placement and data quality. (A) Images of human brains illustrating the position and size of the VOI. (B) Representative ^{1}H STEAM spectra (4 T, 27 mL, T_R = 4.5 s, number of averages = 4) measured at seven T_Es from the human occipital lobe in one young (left) and one elderly (right) subject. The vertical scale has been adjusted such that the NAA resonance detected at T_E = 10 ms for both young and elderly subjects has the same intensity. Horizontal dashed lines are visual guides to indicate that the intensity of NAA and tCr signals decrease faster in the elderly than the young subject. The faster signal decay reflects a shorter T_2 value. Spectra are shown without line broadening. NAA, N-acetylaspartate, tCr, total creatine = creatine (Cr) + phosphocreatine (PCr), tCho, total choline = choline containing compounds.

doi: 10.1371/journal.pone.0077572.g001

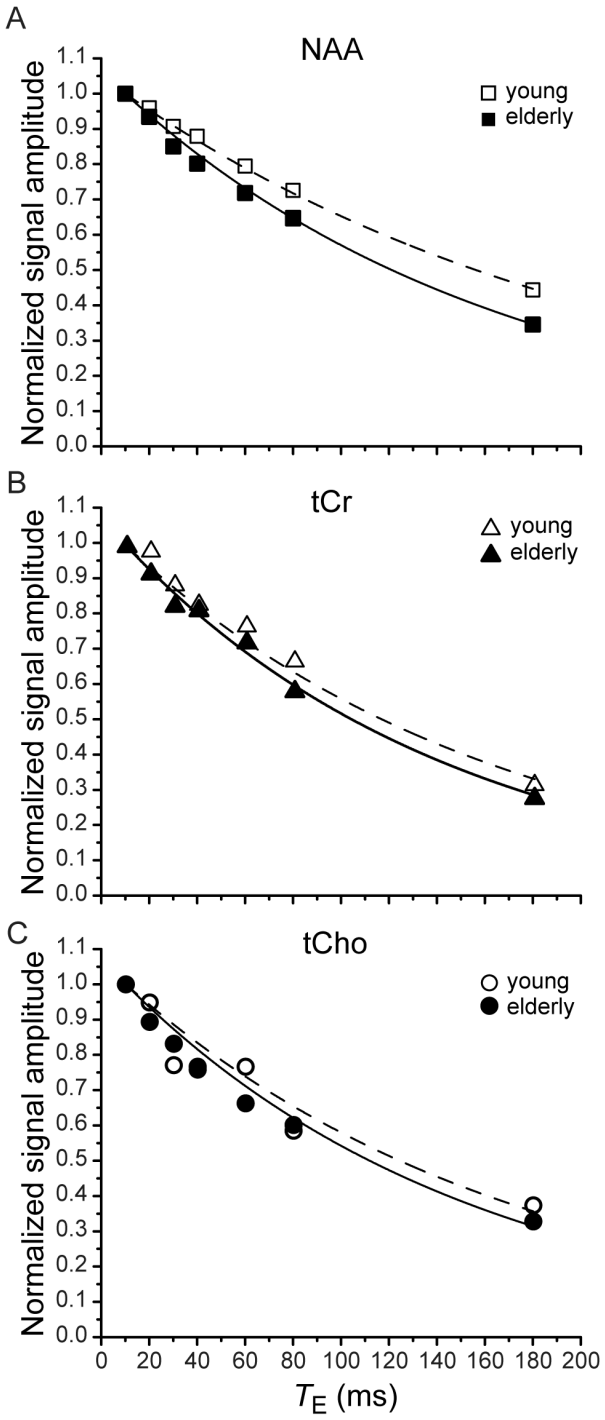

Figure 2. T_2 fits for metabolites in young and elderly subjects. Individual exponential fits (represented by decaying lines) of the experimentally measured data for (A) the NAA singlet at 2.01 ppm, (B) the tCr signal at 3.03 ppm, and (C) the tCho singlet at 3.2 ppm in one representative young and one representative elderly subject. The amplitude of all data sets was normalized by setting the first T_E point to unity for both young and elderly subjects. For all metabolites and all subjects, T_2s were fit with $R^2 \geq 0.918$, with the lowest R^2 for tCho.

doi: 10.1371/journal.pone.0077572.g002

Table 1. T_2 in young and elderly cohorts and summary statistics.

Compound	Young T_2 (ms)	Elderly T_2 (ms)	One-sided probability p	Two-sided probability p	Elderly T_2/Young T_2
NAA	208 ± 18 (252 – 176)	161 ± 19 (200 – 138)	0.00000014	0.00000028	0.77
tCr	157 ± 14 (190 – 138)	132 ± 11 (154 – 120)	0.0000044	0.0000087	0.84
tCho	164 ± 29 (248 – 131)	147 ± 16 (178 – 122)	0.0297	0.059	0.90
Tissue water	52 ± 2 (48 - 57)	47 ± 4 (40 - 51)	0.0000019	0.0000039	0.90

T_2 values (mean ± SD, minimum and maximum values in parenthesis) NAA at 2.01 ppm, tCr at 3.03 ppm, tCho at 3.20 ppm, and tissue water measured in the occipital lobe in 18 young and 14 elderly subjects.

doi: 10.1371/journal.pone.0077572.t001

tissue water was significantly shorter for elderly subjects as compared to young subjects.

For all metabolites and both age groups, the T_2 outcomes from the Monte Carlo simulations preformed with the T_Es utilized experimentally were well within one standard deviation of the T_2 generated utilizing three additional T_Es. The standard deviations of the T_2s simulated using the seven T_Es utilized to measure the *in vivo* data were the same as those achieved experimentally. Lower standard deviations among simulated T_2s were found when any single T_E was added to the data set. The extent of this improvement was similar for addition of either the 120 ms or the 250 ms T_E. The greatest improvement was obtained by including all three extra T_Es (120, 250, and 400 ms).

Discussion

The current results indicate that aging has a significant effect on the T_2 of metabolites, which suggests that this variable may be sensitive to intracellular changes that take place during the neurodegenerative process. Furthermore, this parameter should be considered when studying MRS measured metabolite concentrations among cohorts of differing ages. Although atrophy of the whole brain takes place during aging and CSF content of the VOI was significantly higher for elderly as compared to young subjects, the CSF content of VOI would not influence the measurement of T_2 of metabolites due to the negligible concentration of metabolites in the CSF [32]. The T_2s of all detected intracellular metabolites, NAA, tCr, tCho, and tissue water were shorter in the elderly cohort. The T_2 values of NAA and tCr were significantly different between young and elderly subjects independent of the hypothesis ($p < 0.05$ for both two-sided and one-sided probability distributions). The largest difference was obtained for NAA with 26% shorter T_2 in elderly as compared to young subjects. For tCr, the difference was 16%. Although a 10% shorter T_2 was observed for tCho in elderly as compared to young subjects, this difference was only at the trend level when using a two-sided probability distribution ($p = 0.059$). This is due to large standard deviation among tCho T_2s especially in young cohort. However, the difference was statistically significant under the hypothesis that lower T_2 values will be observed in elderly than young subjects for all metabolites (one-sided probability distribution, $p = 0.03$). The standard deviation is higher for young subjects than elderly subjects due to the poorer fits.

The T_2 measurements were performed in 2.1 minutes which is short enough to be routinely added to any spectroscopic protocol. However, with 4 scans taken at each T_E, it was not possible to obtain T_2 values for metabolites other than NAA, tCr and tCho due to the fact that reliable quantification of other metabolites was not possible at all T_Es. The reliability in quantification of metabolite concentrations increases with increasing SNR [23]. Therefore, additional metabolites such as *m*Ins, Glu and Gln could potentially be quantified with an increased number of scans. Detection of the T_2s of these additional compounds would increase the sensitivity of this approach to changes that take place during the neurodegenerative process.

The Monte Carlo simulations revealed that the same T_2 values as obtained in this study would be measured if more T_Es were added. Therefore, the T_2 values observed for young and elderly subjects were not biased by the T_Es at which spectra were measured. Additionally, Monte Carlo simulations revealed that the standard deviation values that were obtained experimentally were the lowest that could be expected based on the quality of the data used. Acquiring additional spectra at either one or two longer T_Es than those used in this study would lower standard deviations, but not change the group mean T_2. Acquiring this additional data would improve the accuracy of the T_2 measured in each individual. Expected improvement in standard deviations would make findings more significant which would be especially appealing in the case of tCho. As such, the approach would become sensitive to changes in cell viability at an earlier disease stage. Nonetheless, the improvement would come at the cost of extending the measurement time since additional spectra would need to be acquired.

The T_2 values measured in the young subjects were similar to those previously reported at the similar field strength [33–35]. Although the measurements were neither performed with the same methods nor in the same brain region, T_2 values from all these studies are within one standard deviation of each other.

The T_2 values of brain metabolites as a function of age have been measured in several studies at 1.5 or 3 T with contradicting results [10–13]. Our finding of faster T_2s in elderly than young subjects is in agreement with the prior study that is most similar to ours [11]. Both of these studies scanned the occipital lobe, were carried out at similar magnetic field (3 and 4 T), and spanned approximately 60 years of aging (although the study by Christiansen et al. also spanned similar age

range). At lower field, the smaller chemical shift dispersion leads to increased overlap among metabolites, which precludes separation of constituent signal contributions. For example, the NAA signal at 2.01 ppm has contributions from underlying resonances from Glu, Gln, and macromolecules. In the study by Kirov et al., the extent to which T_2 was lower in elderly than adolescent subjects was: 12% for NAA, 10% for tCho, and 6% for tCr. These T_2 values were obtained with a T_E set that was tailored to measuring the ~180 ms T_2. In our study, shorter T_Es were sampled which could be advantageous to extent to which differential information exists in the data at shorter T_Es. Both studies observed the largest difference in T_2 of NAA. They also agree that if a linear decline is assumed, the changes in T_2s are less than 1 ms per year. The other study that was similar to ours in that spectral deconvolution for determination of constituent signal strengths was utilized did not find an age associated difference in the frontal cortex over a shorter age span [13]. The earliest study of this type [10] suffered from an unfortunate combination of utilizing the area under the peak to measure signal strength and persistence of substantial water signal in the metabolite spectra. While utilizing the integral area under the metabolite resonance generally suffers from confounding by overlapping resonances, the persistent substantial water signal may have exacerbated this problem. Finally, our study did not agree with novel study that was designed to measure metabolite concentrations with correction for relaxation rates [12]. Regarding that novel study, the authors cautions that "apparent age-dependence of metabolite T_2s could merely be a reflection of age-dependent changes of signal characteristics of myelin water [12]." They also emphasized that the approach was designed to move toward true absolute quantification by taking into account non-negligible differences in relaxation rates. The approach used for measuring T_2 in that work [12] has not been adopted since its publication. While the importance of considering possible age and disease associated difference in T_2 continues to be emphasized, the need for dedication of additional scanning time to measure spectra at several T_Es is generally acknowledged. Additional studies designed to scan the brain regions and age spans represented in these five studies as well as magnetic field dependence would be needed to further understand the origin of the discrepancies.

The human brain undergoes morphologic and physiological changes over the 50 to 60 years separating the two groups observed in this study. Since atrophy in normal aging involves neuronal shrinkage, as well as axonal and myelin degeneration [36–38], the resulting increase in the fraction of small neurons and reduction in water content could result in shorter T_2 of metabolites [11]. Furthermore, age-dependent iron deposition has shown a strong correlation with T_2 shortening [39,40]. The measurement of T_2 of metabolites is not able to distinguish among these possible causes of T_2 shortening. However, all of the phenomena take place in aging and at a younger age in Alzheimer's disease. The cellular changes and iron accumulation occur regionally with some brain regions highly vulnerable to aging while other brain regions are spared. Therefore the brain region selectivity of this approach renders it highly applicable to for changes that occur in areas that are impacted earliest and to the greatest extent in Alzheimer's diseases. That T_2 differences between young and elderly subjects were found even though the occipital cortex is spared suggests that T_2 measurement is sensitive to small changes in the cellular environment. T_2 differences are expected to be largest in the brain regions that are most vulnerable to neurodegenerative processes.

Conclusions

The findings of this study suggest that noninvasive detection of T_2 provides useful biological information on changes in the cellular microenvironment that take place during aging. As such, brain region specific studies of T_2 relaxation could lead toward discovery of an early stage biomarker, and could enlighten changes that take place during normal and pathological aging. Such studies could be designed to elucidate mechanisms, especially if combined with diffusion weighted spectroscopy and mapping of the regional iron content. T_2 also has potential for development as a tool to monitor efficacy of experimental therapies.

Acknowledgments

We thank Pierre-Gilles Henry, Ph.D. and Ivan Tkac, Ph.D. for helpful discussions, Joanna Lucas, Ph.D. and Stephen D. Weigand, M.S. for help with the statistics, the University of Minnesota Alumni Association and the Metropolitan Area Agency on Aging (MAAA) for assistance in recruiting elderly subjects, and colleagues at CMRR for maintaining spectrometer performance.

Author Contributions

Conceived and designed the experiments: UEE MT. Performed the experiments: UEE DKD. Analyzed the data: UEE MM MT. Contributed reagents/materials/analysis tools: DKD MM UEE. Wrote the manuscript: MM. revised and reviewed manuscript: MT DKD UEE.

References

1. de Graaf RA (2007) In Vivo NMR Spectroscopy. Principles and Techniques. John Wiley & Sons, Ltd.
2. Nicolay K, Braun KP, Graaf RA, Dijkhuizen RM, Kruiskamp MJ (2001) Diffusion NMR spectroscopy. NMR Biomed 14: 94-111. doi:10.1002/nbm.686. PubMed: 11320536.
3. Ross B, Bluml S (2001) Magnetic resonance spectroscopy of the human brain. Anat Rec 265: 54-84. doi:10.1002/ar.1058. PubMed: 11323770.
4. Birken DL, Oldendorf WH (1989) N-acetyl-L-aspartic acid: a literature review of a compound prominent in 1 H-NMR spectroscopic studies of brain. Neurosci Biobehav Rev 13: 23-31. doi:10.1016/S0149-7634(89)80048-X. PubMed: 2671831.
5. Valette J, Guillermier M, Besret L, Hantraye P, Bloch G et al. (2007) Isoflurane strongly affects the diffusion of intracellular metabolites, as shown by 1 H nuclear magnetic resonance spectroscopy of the monkey brain. J Cereb Blood Flow Metab 27: 588-596. doi:10.1038/sj.jcbfm.9600353. PubMed: 16788716.

6. Ongür D, Prescot AP, Jensen JE, Rouse ED, Cohen BM et al. (2010) T_2 relaxation time abnormalities in bipolar disorder and schizophrenia. Magn Reson Med 63: 1-8. PubMed: 19918902.
7. Lei H, Zhang Y, Zhu XH, Chen W (2003) Changes in the proton T2 relaxation times of cerebral water and metabolites during forebrain ischemia in rat at 9.4 T. Magn Reson Med 49: 979-984.
8. Larvaron P, Bielicki G, Boespflug-Tanguy O, Renou JP (2006) Proton MRS of early post-natal mouse brain modifications *in vivo*. NMR Biomed 19: 180-187. doi:10.1002/nbm.997. PubMed: 16470692.
9. Tunc-Skarka N, Weber-Fahr W, Hoerst M, Meyer-Lindenberg A, Zink M et al. (2009) MR spectroscopic evaluation of N-acetylaspartate's T2 relaxation time and concentration corroborates white matter abnormalities in schizophrenia. NeuroImage 48: 525-531. doi:10.1016/j.neuroimage.2009.06.061. PubMed: 19573608.
10. Christiansen P, Toft P, Larsson HB, Stubgaard M, Henriksen O (1993) The concentration of *N*-acetyl aspartate, creatine + phosphocreatine, and choline in different parts of the brain in adulthood and senium. Magn Reson Imaging 11: 799-806. doi:10.1016/0730-725X(93)90197-L. PubMed: 8371635.
11. Kirov I, Fleysher L, Fleysher R, Patil V, Liu S et al. (2008) Age dependence of regional proton metabolites T2 relaxation times in the human brain at 3 T. Magn Reson Med 60: 790-795.
12. Kreis R, Slotboom J, Hofmann L, Boesch C (2005) Integrated data acquisition and processing to determine metabolite contents, relaxation times, and macromolecule baseline in single examinations of individual subjects. Magn Reson Med 54: 761-768. doi:10.1002/mrm.20673. PubMed: 16161114.
13. Brooks JC, Roberts N, Kemp GJ, Gosney MA, Lye M et al. (2001) A proton magnetic resonance spectroscopy study of age-related changes in frontal lobe metabolite concentrations. Cereb Cortex 11: 598-605. doi:10.1093/cercor/11.7.598. PubMed: 11415962.
14. Double KL, Reyes S, Werry EL, Halliday GM (2010) Selective cell death in neurodegeneration: why are some neurons spared in vulnerable regions? Prog Neurobiol 92: 316-329. doi:10.1016/j.pneurobio.2010.06.001. PubMed: 20541584.
15. Wang X, Michaelis ML, Michaelis EK (2010) Functional genomics of brain aging and Alzheimer's disease: focus on selective neuronal vulnerability. Curr Genomics 11: 618-633. doi:10.2174/138920210793360943. PubMed: 21629439.
16. Nasreddine ZS, Phillips NA, Bédirian V, Charbonneau S, Whitehead V et al. (2005) The Montreal Cognitive Assessment, MoCA: a brief screening tool for mild cognitive impairment. J Am Geriatr Soc 53: 695-699. doi:10.1111/j.1532-5415.2005.53221.x. PubMed: 15817019.
17. Onishi J, Suzuki Y, Umegaki H, Endo H, Kawamura T et al. (2006) A comparison of depressive mood of older adults in a community, nursing homes, and a geriatric hospital: factor analysis of Geriatric Depression Scale. J Geriatr Psychiatry Neurol 19: 26-31. doi:10.1177/0891988705284725. PubMed: 16449757.
18. Adriany G, Gruetter R (1997) A half-volume coil for efficient proton decoupling in humans at 4 tesla. J Magn Reson 125: 178-184. doi:10.1006/jmre.1997.1113. PubMed: 9245377.
19. Hennig J, Nauerth A, Friedburg H (1986) RARE imaging: a fast imaging method for clinical MR. Magn Reson Med 3: 823-833. doi:10.1002/mrm.1910030602. PubMed: 3821461.
20. Gruetter R (1993) Automatic, localized *in vivo* adjustment of all first- and second-order shim coils. Magn Reson Med 29: 804-811. doi:10.1002/mrm.1910290613. PubMed: 8350724.
21. Gruetter R, Tkác I (2000) Field mapping without reference scan using asymmetric echo-planar techniques. Magn Reson Med 43: 319-323. doi:10.1002/(SICI)1522-2594(200002)43:2. PubMed: 10680699.
22. Tkáč I, Gruetter R (2005) Methodology of 1 H NMR Spectroscopy of the Human Brain at Very High Magnetic Fields. Appl Magn Reson 29: 139-157. doi:10.1007/BF03166960. PubMed: 20179773.
23. Tkác I, Oz G, Adriany G, Uğurbil K, Gruetter R (2009) In vivo 1H NMR spectroscopy of the human brain at high magnetic fields: metabolite quantification at 4T vs. 7T. Magn Reson Med 62: 868-879. doi:10.1002/mrm.22086. PubMed: 19591201.
24. Tkác I, Starcuk Z, Choi IY, Gruetter R (1999) In vivo 1H NMR spectroscopy of rat brain at 1 ms echo time. Magn Reson Med 41: 649-656. doi:10.1002/(SICI)1522-2594(199904)41:4. PubMed: 10332839.
25. Pfeuffer J, Tkác I, Provencher SW, Gruetter R (1999) Toward an *in vivo* neurochemical profile: quantification of 18 metabolites in short-echo-time 1H NMR spectra of the rat brain. J Magn Reson 141: 104-120. doi:10.1006/jmre.1999.1895. PubMed: 10527748.
26. Provencher SW (1993) Estimation of metabolite concentrations from localized *in vivo* proton NMR spectra. Magn Reson Med 30: 672-679. doi:10.1002/mrm.1910300604. PubMed: 8139448.
27. Provencher SW (2001) Automatic quantitation of localized *in vivo* 1H spectra with LCModel. NMR Biomed 14: 260-264. doi:10.1002/nbm.698. PubMed: 11410943.
28. Henry PG, Marjanska M, Walls JD, Valette J, Gruetter R et al. (2006) Proton-observed carbon-edited NMR spectroscopy in strongly coupled second-order spin systems. Magn Reson Med 55: 250-257. doi:10.1002/mrm.20764. PubMed: 16402370.
29. Govindaraju V, Young K, Maudsley AA (2000) Proton NMR chemical shifts and coupling constants for brain metabolites. NMR Biomed 13: 129-153. doi:10.1002/1099-1492(200005)13:3. PubMed: 10861994.
30. Kaiser LG, Marjańska M, Matson GB, Iltis I, Bush SD et al. (2010) H MRS detection of glycine residue of reduced glutathione in vivo 1. J Magn Reson 202: 259-266 doi:10.1016/j.jmr.2009.11.013. PubMed: 20005139.
31. Ernst T, Kreis R, Ross BD (1993) Absolute Quantitation of Water and Metabolites in the Human Brain. 1. Compartments and Water. J Magn Reson B 102: 1-8. doi:10.1006/jmrb.1993.1055.
32. Kruse T, Reiber H, Neuhoff V (1985) Amino acid transport across the human blood-CSF barrier. An evaluation graph for amino acid concentrations in cerebrospinal fluid. J Neurol Sci 70: 129-138. doi:10.1016/0022-510X(85)90082-6. PubMed: 4056818.
33. Hetherington HP, Mason GF, Pan JW, Ponder SL, Vaughan JT et al. (1994) Evaluation of cerebral gray and white matter metabolite differences by spectroscopic imaging at 4.1T. Magn Reson Med 32: 565-571. doi:10.1002/mrm.1910320504. PubMed: 7808257.
34. Posse S, Cuenod CA, Risinger R, Le Bihan D, Balaban RS (1995) Anomalous transverse relaxation in 1 H spectroscopy in human brain at 4 Tesla. Magn Reson Med 33: 246-252. doi:10.1002/mrm.1910330215. PubMed: 7707916.
35. Michaeli S, Garwood M, Zhu XH, DelaBarre L, Andersen P et al. (2002) Proton T2 relaxation study of water, N-acetylaspartate, and creatine in human brain using Hahn and Carr-Purcell spin echoes at 4T and 7T. Magn Reson Med 47: 629-633.
36. Dickstein DL, Kabaso D, Rocher AB, Luebke JI, Wearne SL et al. (2007) Changes in the structural complexity of the aged brain. Aging Cell 6: 275-284. doi:10.1111/j.1474-9726.2007.00289.x. PubMed: 17465981.
37. Bishop NA, Lu T, Yankner BA (2010) Neural mechanisms of ageing and cognitive decline. Nature 464: 529-535. doi:10.1038/nature08983. PubMed: 20336135.
38. Peters A (2002) The effects of normal aging on myelin and nerve fibers: a review. J Neurocytol 31: 581-593. doi:10.1023/A:1025731309829. PubMed: 14501200.
39. Mitsumori F, Watanabe H, Takaya N (2009) Estimation of brain iron concentration in vivo using a linear relationship between regional iron and apparent transverse relaxation rate of the tissue water at 4.7T. Magn Reson Med 62: 1326-1330. doi:10.1002/mrm.22097. PubMed: 19780172.
40. Schenker C, Meier D, Wichmann W, Boesiger P, Valavanis A (1993) Age distribution and iron dependency of the T2 relaxation time in the globus pallidus and putamen. Neuroradiology 35: 119-124. doi:10.1007/BF00593967. PubMed: 8433786.